

Hydro-Magnetic Mixed Convection Double Diffusive in a Lid Driven Square Cavity

Mohamed M. Khairat Dawood

Faculty of Engineering, Suez Canal University, Ismailia, Egypt
E-mail: khairat4975@yahoo.com

Mohamed A. Teamah

*Mechanical Engineering Department, Faculty of Engineering
Alexandria University, Egypt, Currently, Visiting Professor
Faculty of Engineering and Technology
Arab Academy for Science and Technology and Maritime Transport
Alexandria, Egypt*
E-mail: mteamah@yahoo.com

Abstract

The hydro-magnet double diffusive mixed convection in a square lid-driven cavity is studied numerically. Constant temperatures and concentration are imposed along the vertical sides of the square enclosure. Both upper and lower surfaces are being insulated and impermeable. The lid is assumed to be moving in two directions that aids or opposes the free convection. In addition, a uniform magnetic field is applied in a horizontal direction. Results are presented for different values of Hartmann number ($0 \leq Ha \leq 50$), Richardson number ($0.01 \leq Ri \leq 10$) and buoyancy ratio, $-10 \leq N \leq 10$. This study is done for constant Prandtl number, $Pr = 0.7$, Lewis number, $Le = 2$ and the Grashof number, $Gr = 10^4$. The numerical results studied the effect of Richardson number, Hartmann number and buoyancy ratio on the local values (iso-contours of stream line, temperature, concentration as well as both local Nusselt and Sherwood numbers). In addition, the predicted results for both average Nusselt and Sherwood numbers are presented and discussed for various parametric conditions. It is found that direction of lid is more effective on heat and mass transfer and fluid flow with increasing of magnetic field for all studied parameters

Keywords: Laminar mixed convection; Lid-driven; Magnetic field; Thermal and mass diffusion

1. Introduction

Mixed convection heat transfer and fluid flow in square cavities with moving lid are important subjects of investigation due to their effect on many engineering applications as the cooling of electronic systems, nuclear reactors, chemical processing equipment, lubricating grooves, solar collectors, crystal growth and food processing. The Combined temperature and concentration buoyancy force is Called double-diffusion. Double-Diffusion occurs in a very wide range of applications such as oceanography, astrophysics, geology, biology, and chemical processes, as well as in many engineering

applications such as solar ponds, natural gas storage tanks, crystal manufacturing, and metal solidification processes. Lee and Hyun [1] compared their results with reported experimental results for double-diffusive convection in a rectangular enclosure with aiding and opposing temperature and concentration gradients. Al-Amiri et al. [2] investigated numerically steady mixed convection in a square lid-driven cavity under the combined buoyancy effects of thermal and mass diffusion. The heat and mass transfer rates were examined using several operational dimensionless parameters, such as the Richardson number Ri , Lewis number Le and buoyancy ratio parameter N . The average Nusselt and Sherwood numbers are obtained at the bottom wall for some values of the parameters considered in this investigation. The results demonstrate the range where high heat and mass transfer rates can be attained for a given Richardson number. Sharif [3] studied numerically laminar mixed convective heat transfer in two-dimensional shallow rectangular driven cavities of aspect ratio 10. The top moving lid of the cavity is at a higher temperature than the bottom wall. The effects of inclination of the cavity on the flow and thermal fields are investigated. The stream line and isotherm plots and the variation of the local and average Nusselt numbers at the hot and cold walls are presented. Chen and Cheng [4] investigated numerically the Periodic behavior of the mixed convective flow in a rectangular cavity with a vibrating lid. The periodic flow patterns and heat transfer characteristics found are discussed with attention being focused on the interaction between the frequency of the lid velocity vibration and the frequency of the natural periodic flow. Khanafer et al. [5] investigated numerically unsteady laminar mixed convection heat transfer in a lid driven cavity. The forced convective flow inside the cavity is attained by a mechanically induced sliding lid, which is set to oscillate horizontally in a sinusoidal fashion. The natural convection effect is sustained by subjecting the bottom wall to a higher temperature than its top counterpart. In addition, the two vertical walls of the enclosure are kept insulated. Fluid flow and heat transfer characteristics are examined in the domain of the Reynolds number, Grashof number and the dimensionless lid oscillation frequency. Rahman et al. [6] investigated numerically the conjugate effect of joule heating and magnetic force, acting normal to the left vertical wall of an obstructed lid-driven cavity saturated with an electrically conducting fluid. The cavity is heated from the right vertical wall isothermally. Temperature of the left vertical wall, which has constant flow speed, is lower than that of the right vertical wall. Horizontal walls of the cavity are adiabatic. Results were presented in terms of streamlines, isotherms, average Nusselt number at the hot wall and average fluid temperature in the cavity for the magnetic parameter, Ha and Joule heating parameter J . The results showed that the obstacle has significant effects on the flow field at the pure mixed convection region and on the thermal field at the pure forced convection region. Oztop et al. [7] studied numerically Laminar mixed convection flow in the presence of magnetic field in a top sided lid-driven cavity heated by a corner heater. The corner heater is under isothermal boundary conditions with different length in bottom and right vertical walls. Finite volume technique was used to solve governing equations. The temperature of the lid is lower than that of heater. The study is performed for different Grashof and Hartmann numbers at $Re = 100$. Chamkha [8] made a numerical work on hydro-magnetic combined convection flow in a lid-driven cavity with internal heat generation using finite volume approach. The presence of the internal heat generation effects was found to decrease the average Nusselt number significantly for aiding flow and to increase it for opposing flow. Sivasankaran et al. [9] studied numerically the mixed convection in a square cavity of sinusoidal boundary temperatures at the side walls in the presence of magnetic field. In their case, the horizontal walls of the cavity are adiabatic. They indicated that the flow behavior and heat transfer rate inside the cavity are strongly affected by the presence of the magnetic field. Cheng [10] investigated numerically mixed convection in a 2-D lid-driven square cavity to characterize the heat transfer behavior and to validate the Nusselt number (Nu) correlations reported in the literature. The two vertical walls of the cavity are adiabatic while the top moving-wall and the bottom wall are maintained isothermal but the temperature of the bottom wall is higher than that of the top moving-wall. This investigation covers a wide range of Reynolds number (Re) which is varied from 10 to 2200, and the Grashof number (Gr) is varied proportionally to Reynolds number so that Richardson number (Ri) is remained constant. Computed average Nusselt number at the hot bottom wall indicates that the heat transfer increases continuously

with increasing both Re and Gr for $Ri = 0.01$ but is not for $0.5 < Ri < 100$. A sudden drop of Nusselt number is observed at $Re = 713, 376, 248, 129,$ and 61 for $Ri = 0.5, 1, 2, 10,$ and 100 , respectively, due to the change of flow and thermal structures, heat transfer mechanism, and kinetic energy. Ozoe and Maruo [11] investigated magnetic and gravitational natural convection of melted silicon two-dimensional numerical computations for the rate of heat transfer. Cheng and Liu [12] investigated numerically the effect of temperature gradient orientation on the fluid flow and heat transfer in a lid-driven differentially heated square cavity. Four cases were considered depending on the direction of temperature gradient imposed. The differentially heated top and bottom walls result in gravitationally stable and unstable temperature gradients. While the differentially heated left and right side walls lead to assisting and opposing buoyancy effects. It was found that both Richardson number and direction of temperature gradient affect the flow patterns, heat transport processes, and heat transfer rates in the cavity. Mohamad and Viskanta [13, 14] performed numerical and experimental study on two- and three-dimensional laminar mixed convection flows in a bottom wall heated shallow driven cavity filled with water or liquid gallium. They reported that the two-dimensional heat transfer results compare favorably with those based on a three-dimensional model for $Gr/Re^2 < 1$. Teamah [15] made a parametric study and an extension for Chamkha and Al-Naser [16, 17] study. A range for thermal Rayleigh number is studied from 10^3 to 10^6 . In addition, a strong magnetic field required for modern electronic devices is considered in this study. For this reason the Hartmann number is increased to 200. Also, the heat generation and absorption coefficients ranged from -50 to $+25$. Moreover, the buoyancy ratio varied from -10 to $+10$. Ma [18] also made an extension for Chamkha and Al-Naser [16] study by developing a temperature-concentration lattice Bhatnagar-Gross-Krook (TCLBGK) model, with a robust boundary scheme for simulating the two-dimensional, hydro-magnetic, double-diffusive convective flow of a binary gas mixture in a rectangular enclosure. The numerical results were found to be in good agreement with those of Chamkha and Al-Naser [17]. Teamah et al. [19] investigated numerically double-diffusive convective flow in an inclined rectangular enclosure with the shortest sides being insulated and impermeable is investigated numerically. In addition, a uniform magnetic field is applied in a horizontal direction. The numerical results are reported for the effect of thermal Rayleigh number on the contours of streamline, temperature, and concentration. In addition, results for the average Nusselt and Sherwood numbers are presented and discussed for various parametric conditions. This study is done for constant Prandtl number, $Pr = 0.7$; aspect ratio, $A = 2$ and Lewis number, $Le = 2$. Computations are carried out for thermal Rayleigh number ranging from 10^3 to 5×10^5 , inclination angle range of $0^\circ \leq \gamma \leq 180^\circ$, dimensionless heat generation and absorption coefficients range of $-40 \leq \Phi \leq 40$, buoyancy ratio range of $-5 \leq N \leq 5$ and the Hartmann number range of $0 \leq Ha \leq 70$. Recently, the attention has been paid to use the magnetic field to enhance or decrease the heat and mass transfer in cavities of different geometries, different inclinations, also it can be filled with porous media or nano-fluid [20-28]. From the previous review it is denoted that the recent researches in heat and mass transfer is very limited and so, our concern in this study is to analyze the double-diffusive convective flow to add a view for the problem for different parameters affect this phenomena.

2. Mathematical Model

The schematic of the system under consideration is shown in Fig. 1. The temperatures T_h and T_c are uniformly imposed along the vertical walls. The top and bottom surfaces are assumed to be adiabatic and impermeable. The left wall is the source for both heat and mass. The enclosure is filled with air. The fluid in this enclosure is assumed to be incompressible, Newtonian, The Boussinesq approximation equation (1) with opposite and compositional buoyancy forces is used for the body force terms in the momentum equations.

$$\rho = \rho_o \left[1 - \beta_T (T - T_c) - \beta_S (c - c_c) \right] \quad (1)$$

$$\frac{\partial u}{\partial x} + \frac{\partial v}{\partial y} = 0 \quad (2)$$

$$\left(u \frac{\partial u}{\partial x} + v \frac{\partial u}{\partial y} \right) = -\frac{1}{\rho} \frac{\partial p}{\partial x} + \nu \left(\frac{\partial^2 u}{\partial x^2} + \frac{\partial^2 u}{\partial y^2} \right) \quad (3)$$

$$\left(u \frac{\partial v}{\partial x} + v \frac{\partial v}{\partial y} \right) = -\frac{1}{\rho} \frac{\partial p}{\partial y} + \nu \left(\frac{\partial^2 v}{\partial x^2} + \frac{\partial^2 v}{\partial y^2} \right) + g \left[\beta_T (T - T_c) - \beta_s (c - c_c) \right] - \frac{\sigma B}{\rho} \quad (4)$$

$$\left(u \frac{\partial T}{\partial x} + v \frac{\partial T}{\partial y} \right) = \alpha \left(\frac{\partial^2 T}{\partial x^2} + \frac{\partial^2 T}{\partial y^2} \right) \quad (5)$$

$$\left(u \frac{\partial c}{\partial x} + v \frac{\partial c}{\partial y} \right) = D \left(\frac{\partial^2 c}{\partial x^2} + \frac{\partial^2 c}{\partial y^2} \right) \quad (6)$$

The boundary conditions for the problem could be written as

- At $x = 0$, $u = v = 0.0$, $T = T_h$ and $c = c_h$
- At $x = L$, $u = v = 0.0$, $T = T_c$ and $c = c_c$
- at $y = 0$, $u = v = \frac{\partial T}{\partial y} = \frac{\partial c}{\partial y} = 0.0$
- and $y = L$; $u = \pm u_0$, $v = \frac{\partial T}{\partial y} = \frac{\partial c}{\partial y} = 0.0$ (7)

When the upper surface moves to right direction its velocity will be positive. On the other hand if it moves to left direction its velocity will be negative.

The boundary conditions and the governing equations are non dimensionalized using the following dimensionless variables

$$X = \frac{x}{L}, Y = \frac{y}{L}, U = \frac{u}{u_0}, V = \frac{v}{u_0}, P = \frac{p}{\rho u_0^2}, \theta = \frac{T - T_c}{T_h - T_c}, C = \frac{c - c_c}{c_h - c_c} \quad (8)$$

In the governing equations, the dimensionless governing equations become

$$\frac{\partial U}{\partial X} + \frac{\partial V}{\partial Y} = 0 \quad (9)$$

$$U \frac{\partial U}{\partial X} + V \frac{\partial U}{\partial Y} = -\frac{\partial P}{\partial X} + \frac{1}{\text{Re}} \left(\frac{\partial^2 U}{\partial X^2} + \frac{\partial^2 U}{\partial Y^2} \right) \quad (10)$$

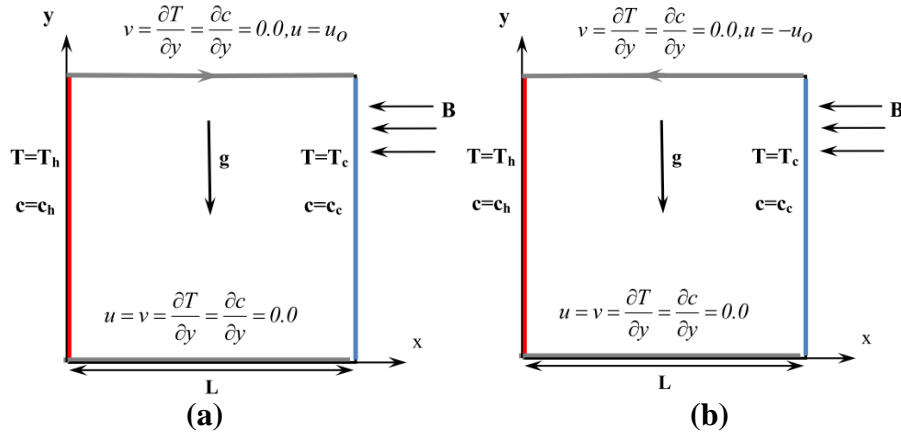
$$U \frac{\partial V}{\partial X} + V \frac{\partial V}{\partial Y} = -\frac{\partial P}{\partial Y} + \frac{1}{\text{Re}} \left(\frac{\partial^2 V}{\partial X^2} + \frac{\partial^2 V}{\partial Y^2} \right) + \frac{Gr}{\text{Re}^2} (\theta + NC) + Ha^2 \text{Pr} V \quad (11)$$

$$U \frac{\partial \theta}{\partial X} + V \frac{\partial \theta}{\partial Y} = \frac{1}{\text{Re Pr}} \left(\frac{\partial^2 \theta}{\partial X^2} + \frac{\partial^2 \theta}{\partial Y^2} \right) \quad (12)$$

$$U \frac{\partial C}{\partial X} + V \frac{\partial C}{\partial Y} = \frac{1}{\text{Le Re Pr}} \left(\frac{\partial^2 C}{\partial X^2} + \frac{\partial^2 C}{\partial Y^2} \right) \quad (13)$$

Where, Pr is the Prandtl number, N is the buoyancy ratio, $\left[\beta_s (C_h - C_c) / \beta_T (T_h - T_c) \right]$, Ha is the Hartmann number = $BL \sqrt{\sigma / \mu}$, and Le is the Lewis number, $\text{Le} = \alpha / D$.

Figure 1: Schematic diagram for the problem with boundary conditions (a) upper surface move to right and (b) upper surface move to left.



The dimensionless boundary conditions for vertical walls are;

- $U = V = 0, \theta = 1, C = 1, \text{At } X = 0$
- $U = V = 0, \theta = 0, C = 0, \text{At } X = 1$

The horizontal boundaries are

- $\text{At } Y = 0, U = V = \frac{\partial \theta}{\partial Y} = \frac{\partial C}{\partial Y} = 0.0$
- $\text{At } Y = 1, V = \frac{\partial \theta}{\partial Y} = \frac{\partial C}{\partial Y} = 0.0, U = \pm 1 \quad (14)$

2.1. Nusselt Number Calculation

Equating the heat transfer by convection to the heat transfer by conduction at hot wall;

$$h \Delta T = -k \left(\frac{\partial T}{\partial x} \right)_{x=0} \quad (15)$$

Introducing the dimensionless variables, defined in equation (8), into equation (15), gives:

$$Nu_l = - \left(\frac{\partial \theta}{\partial X} \right)_{X=0} \quad (16)$$

The average Nusselt number is obtained by integrating the above local Nusselt number over the vertical hot wall:

$$Nu = - \frac{1}{A} \int_0^A \left(\frac{\partial \theta}{\partial X} \right)_{X=0} dY \quad (17)$$

2.2. Sherwood Number Calculation

Equating the extracted mass transfer by convection to the added mass transfer to the cavity gives:

$$h_s \Delta c = -D \left(\frac{\partial c}{\partial x} \right)_{x=0} \quad (18)$$

Introducing the dimensionless variables, defined in equation (8) into equation (18) gives:

$$Sh = - \left(\frac{\partial C}{\partial X} \right)_{X=0} \quad (19)$$

The average Sherwood number is obtained by integrating the above local Sherwood number over the vertical wall:

$$Sh_{avr} = - \frac{1}{A} \int_0^A \left(\frac{\partial C}{\partial X} \right)_{X=0} dY \quad (20)$$

3. Numerical Method

The governing equations are solved using the finite volume technique developed by Patankar [29]. This technique is based on the discretization of the governing equations using the central difference in space. Firstly, the number of nodes used was checked. Three grid sizing were checked (30×30), (60×60) and (100×100). The deviations between the results for local Nusselt number on the left vertical wall obtained for domain (60×60) and (100×100) were less than 0.5%, Fig. 2. Therefore, throughout this study, the number of nodes (60×60) was used. The 60 gridpoints in X-direction were enough to resolve the thin boundary layer near the vertical walls. The discretization equations were solved by the Gauss Seidel method. The iteration method used in this program is a line-by-line procedure, which is a combination of the direct method and the resulting Tri Diagonal Matrix Algorithm (TDMA). The convergence of the iteration is determined by the change in the average Nusselt number as well as other dependent variables through one hundred iterations to be less than 1.2% from its initial value.

4. Program Validation and Comparison with Previous Work

In order to check on the accuracy of the numerical technique employed for the solution of the problem considered in the present study, the code is validated with Al-Amiri et al. [2] by performing simulation for mixed convection flow in a vertical square enclosure with the temperatures T_h and T_c are uniformly imposed along the lower and upper walls respectively as well as concentrations. The vertical walls are assumed to be adiabatic and impermeable while the upper surface is moving right. Streamlines and isotherms are plotted in Fig. 3. showing good agreement.

Figure 2: Effect of grid sizing on local Nusselt number, $Ri=1$, $Ha=25$, $N=1$, and $Le=2$ in case of adding flow

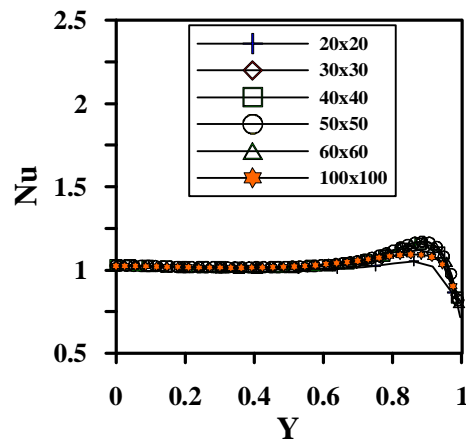
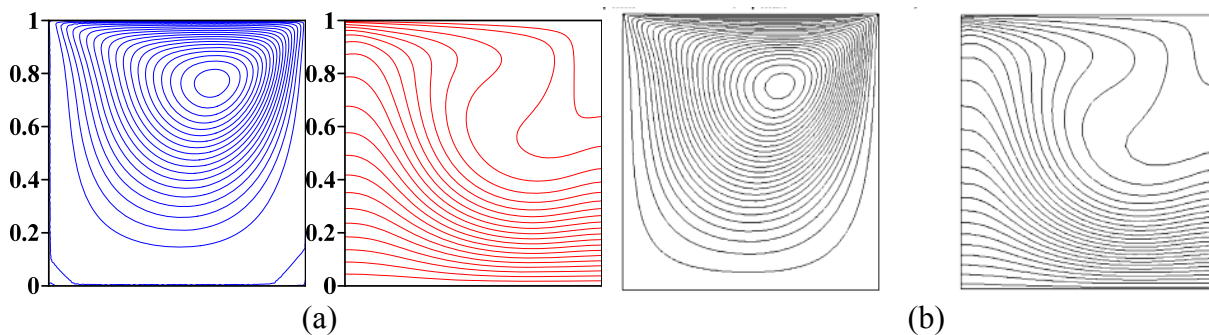


Figure 3: Stream lines, isotherms and iso-concentration for, $Pr=1$, $Ri=0.01$, $Le=10$ and $Ha=0$ (a) present code (b) Al-Amiri et al. [2].



5. Results and Discussions

The effect of both Richardson and Hartmann numbers as well as the buoyancy ratio on double-diffusive mixed convection in a lid-driven square enclosure are examined. In the present study, the Prandtl number, Pr is kept constant at $Pr = 0.7$, Lewis number, $Le = 2$. The governing parameters in mixed convection is Richardson number, $Ri = Gr/Re^2$, which characterizes the relative importance of natural to forced convection, also the buoyancy ratio is studied with both positive and negative values i.e. (assisting and opposing flow). When the upper plate is moving to right, so it is assisted the natural convection from hot side to cold one. Conversely, when the plate moves to left, it opposes the natural convection from hot side to the cold one. The Grashof number is kept constant at 10^4 and Reynolds number is varied by varying the lid velocity u_0 , to achieve the required Richardson number. This study covers ranges of Richardson number from 0.01 to 10, Hartmann number from 0 to 50 and buoyancy ratio from -10 to 10, in the two directions (right and left) for the upper moving plate.

5.1. Effect of Richardson Number

5-1-1 Moving to Right (Adding Flow)

For the upper surface moves to right, the effect of varying Richardson number Ri on the transport phenomena is shown in Fig. 4.

For $Ri = 0.01$, the patterns of flow in clockwise direction due to the support of the forced convection for both positive buoyancy number ($N = 1$) and natural convection from hot left wall to cold right wall. The isothermal, Iso-concentration lines are denser at the upper part of left wall as a result of the forced convection forming thinner boundary layers which causes steep temperature and concentration gradients in the horizontal direction near the left wall increasing in heat and mass transfer. As, Ri is increased to 10, the cavity is in a quasi-conduction domain, i.e., most of the heat transfer occurs due to conduction except near the upper part of the left wall.

Fig. 5 represents local Nusselt and Sherwood numbers for the upper surface moves to right, as Ri decreases, both local Nusselt and Sherwood numbers increase. The local Nusselt and Sherwood numbers increase significantly at the upper left side of the cavity due to thinner boundary layers which cause steep temperature gradients in the horizontal direction near the upper left wall and hence increasing in heat and mass transfer as the Richardson number decreased. At $Ri=10$, where the natural convection is dominated, the local Nusselt and Sherwood decrease gradually with the vertical wall length.

5.1.2. Moving to Left

For the upper surface moves to left, the influence of varying Richardson number Ri on the transport phenomena is shown in Fig. 6. For $Ri = 0.01$, flow patterns are characterized by a recirculating counter clockwise vortex that occupies the upper portion of the cavity due to the effect of forced convection generated by surface moving to left. As $Ri=10$, a major vortex forms near the bottom of cavity due to natural convection effect.

The isothermal, iso-concentration lines are inclined more towards the moving plate to left as a result of the forced convection forming thinner boundary layers which causes steep temperature gradients in the horizontal direction near the left wall near the moving plate and hence increasing in heat and mass transfer. As Richardson number increased, the isothermal and iso-concentration lines are less dense at the upper left wall but much denser than the case of moving plate to Right especially at mixed convection.

Fig. 7 represents local Nusselt and Sherwood numbers for the upper surface moves to Left, as Ri increases both local Nusselt and Sherwood numbers increase slightly in the lower part of the left vertical side as the effect of forced convection decreases, causing the isothermal and isoconcentration lines to get close to vertical wall which increase the temperature and concentration gradient. Both local Nusselt and Sherwood numbers increase as Ri decreases at the upper left side of the cavity due to

thinner boundary layers which cause steep temperature gradients in the horizontal direction near the upper left wall and hence increasing in heat and mass transfer.

Fig.8.Show important comparison to for the average Nusselt and Sherwood at $Pr=0.7$, $Ha=0, N=1$) for the direction of the plate. When lid moves in $-x$ direction, the fluid impinges to the left vertical wall and separates to two parts. For moving lid in $-X$ direction, double cells were formed inside the cavity. Isotherms and Iso-concentration are affected by these eddies. It means that natural convection is effective in that region which increased the heat and mass transfer in the $-x$ direction than positive direction.

Figure 4: Effect of Richardson number on stream line, isothermals and isoconcentration (upper surface moves to right, $Pr = 0.7$, $Le = 2$, $N = 1$ and $Ha=0$).

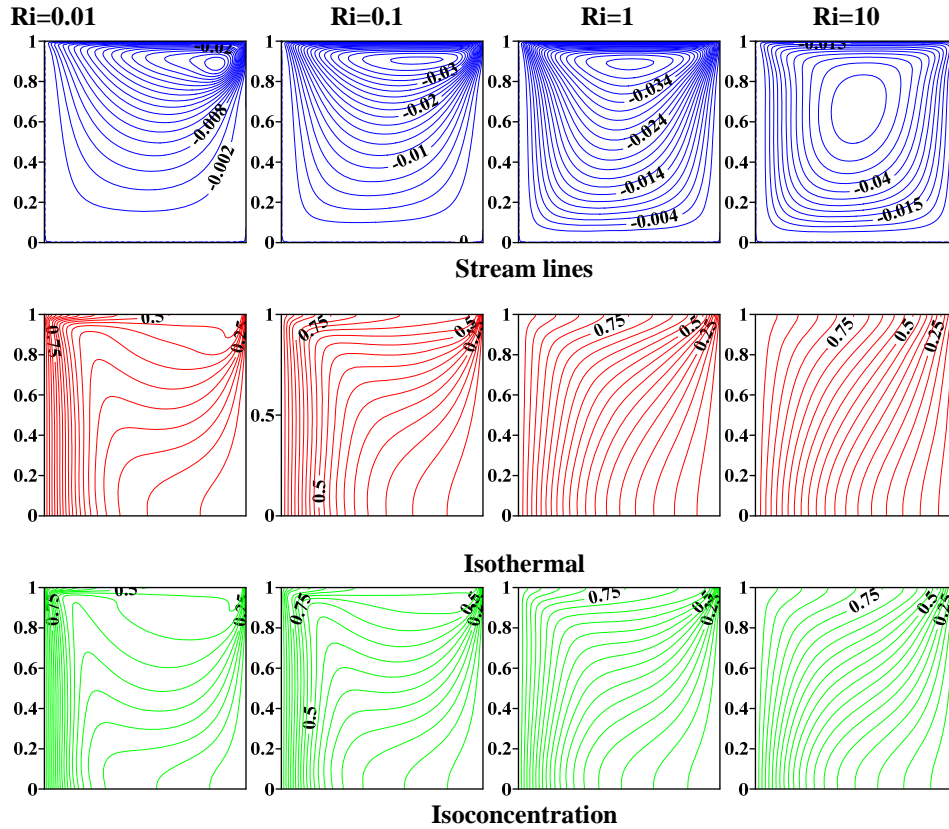


Figure 5: Effect of Richardson number for (upper surface moves to right, $Pr = 0.7$, $Le = 2$, $N = 1$ and $Ha=0$) on (a) Local Nusselt number (b) Local Sherwood number

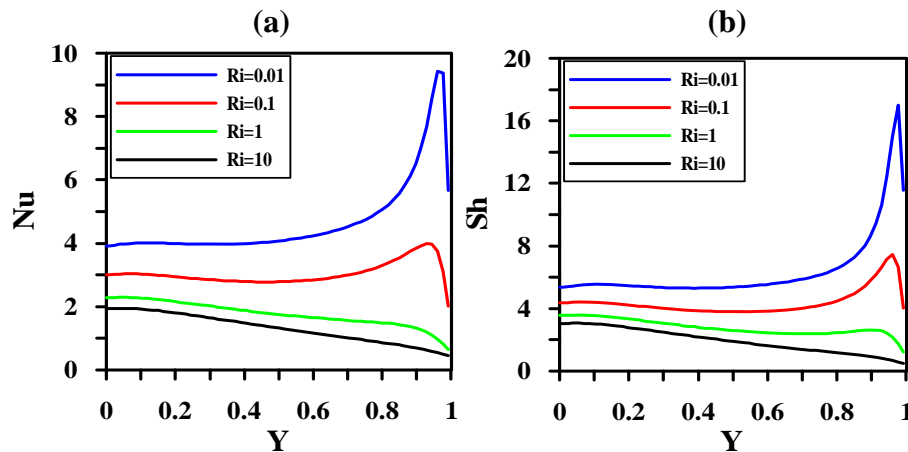
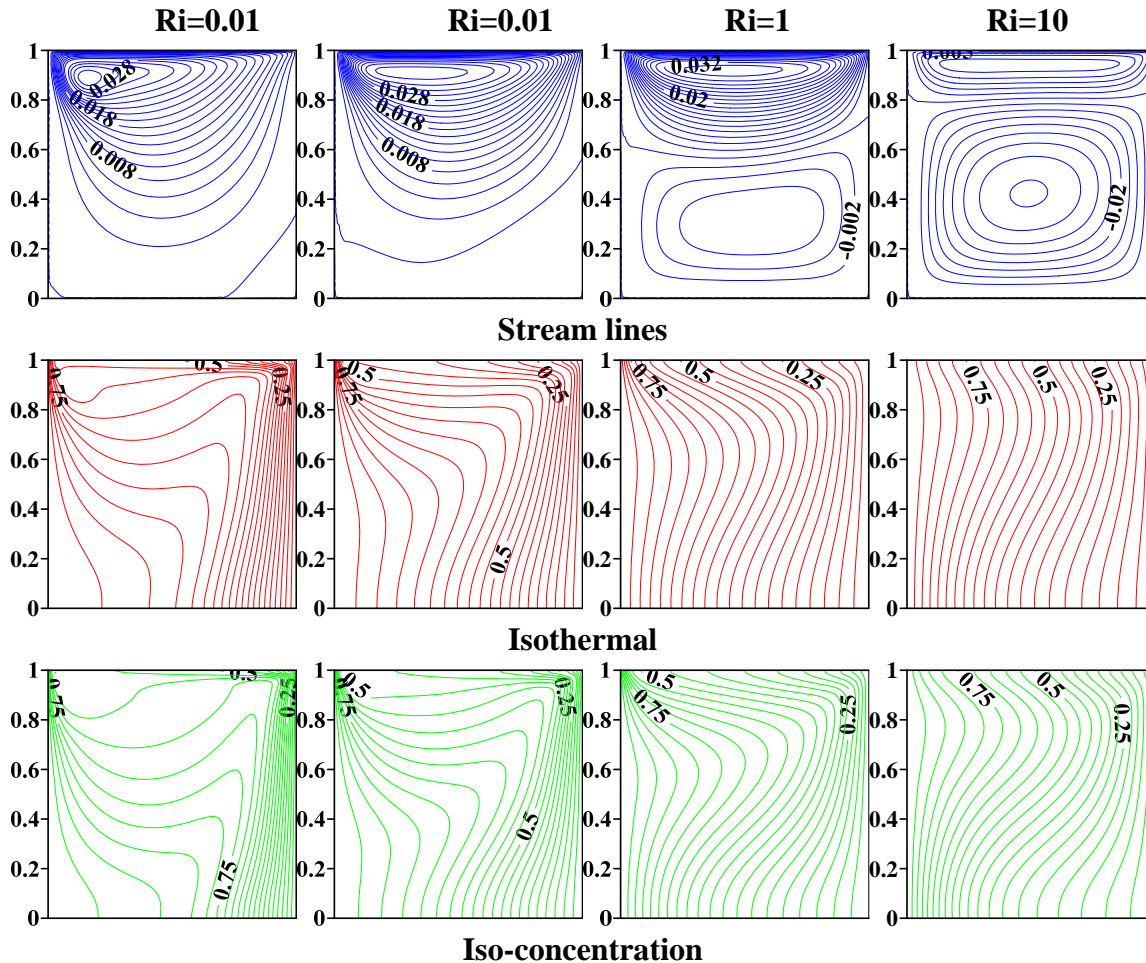


Figure 6: Effect of Richardson number on stream line, isothermals and iso-concentration (upper surface moves to left, $Pr = 0.7$, $Le = 2$, $N = 1$ and $Ha=0$).



5.2. Effect of Hartmann Number

5.2.1. Lid Moving to Right

Fig.9. illustrate the stream ,isotherms and iso-concentration lines for $Ri=1$,while the Hartmann number attains the values 0,10,30 and 50, respectively.The flow behavior is affected along with the change in the Hartmann number. In the absence of magnetic field, the flow is characterized by a single circulating vortex inside the enclosure. Since the applied magnetic field has the tendency to slow down the movement of the fluid in the cavity, the flow circulation inhibit gradually except in the region close to the moving top wall of the cavity. In other words, when the Hartmann number is increased, the circulation in the flow is progressively restricted to the region at the top of the cavity. As increasing the Hartmann the isothermal and iso-concentration lines are parallel to the vertical walls .As and hence the conduction regime is highly dominant.

Fig. 10 represents the local Nusselt and Sherwood numbers when the upper surface moves to right direction. In the absence of magnetic field, as the local Nusselt and Sherwood number have maximum values at the cavity bottom and its value decreases as moving upwards. As Ha increases both local Nusselt and Sherwood numbers decreases, but the maximum value occur near the upper moving surface the cavity due to thinner boundary layers which cause steep temperature and concentration gradients in the horizontal direction near the upper left wall and hence increasing in heat and mass transfer.

Figure 7: Effect of Richardson number for (upper surface moves to left, $Pr = 0.7$, $Le = 2$, $N = 1$ and $Ha=0$) on (a) Local Nusselt number (b) Local Sherwood number

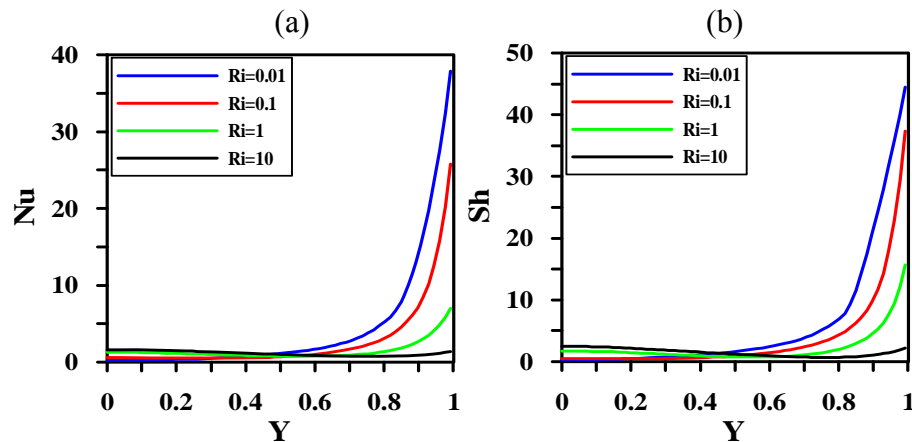
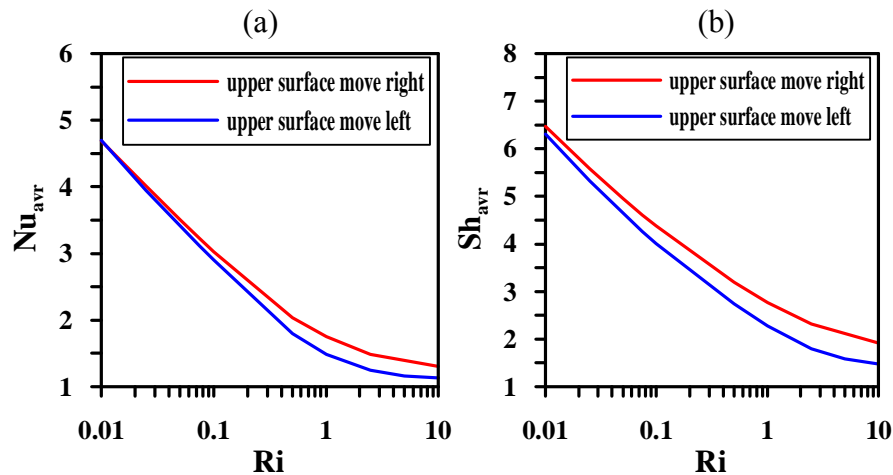


Figure 8: Effect of Richardson number for ($Pr = 0.7$, $Le = 2$, $N = 1$ and $Ha=0$) on (a) average Nusselt number (b) average Sherwood number



5.2.2. Lid Moving to Left (Opposing Flow)

Fig. 11 shows that the flow behavior is affected along with the change in the Hartmann number. In the absence of magnetic field, the flow is characterized by two circulating vortex inside the enclosure. Since the applied magnetic field, the flow circulation inhibit gradually except in the region close to the moving top wall of the cavity. The same observation as moving to right, as increasing the Hartmann the isothermal and iso-concentration lines are parallel to the vertical walls. As and hence the conduction regime is highly dominant.

Fig.12 represent the local Nusselt and Sherwood numbers for the upper surface move to left. In the absence of magnetic field, the local Nusselt and Sherwood number increase in the region near the upper surface due to the effect of forced convection. As Ha increases, both local Nusselt and Sherwood numbers decreases near the upper surface. The effect of Ha on the local Nusselt and Sherwood numbers at the rest of the cavity is not significant.

5.2.3. Average Nusselt and Sherwood Number for Adding and Opposing Flow

Figs. 13 and 14 plots the effect of Hartmann number on the average Nusselt and Sherwood numbers to emphasize the effect of applying magnetic field to the cavity's shown in the figure the magnetic field effect is to suppress the heat and mass transfer within the cavity by decreasing the average Nusselt number and Sherwood numbers. Since a transverse magnetic field is applied in the horizontal direction

normal to the vertical walls of the cavity, a resistive force occurs. Consequently, the horizontal velocity component of the cavity decreases. So, the average Nusselt and Sherwood number for the case of plate moves left is higher than moving right as Ha increased.

Figure 9: Effect of Hartman number on stream line, isothermals and isoconcentration (upper surface moves to Right ($Pr = 0.7, Le = 2, N = 1$ and $Ri=1$)).

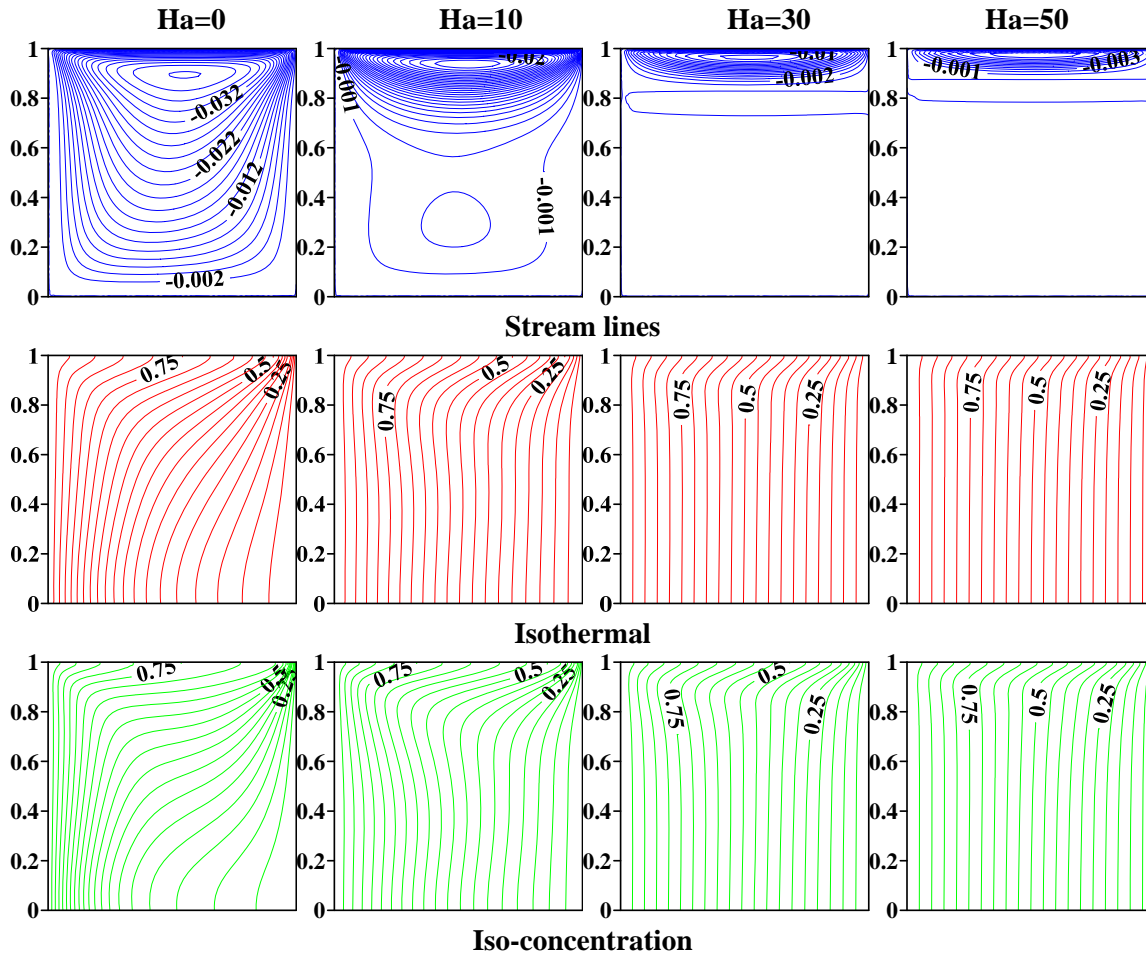


Figure 10: Effect of Hartmann number for (lid moves to right, $Pr = 0.7, Le = 2, N = 1$ and $Ri=1$) on (a) Local Nusselt number (b) Local Sherwood number

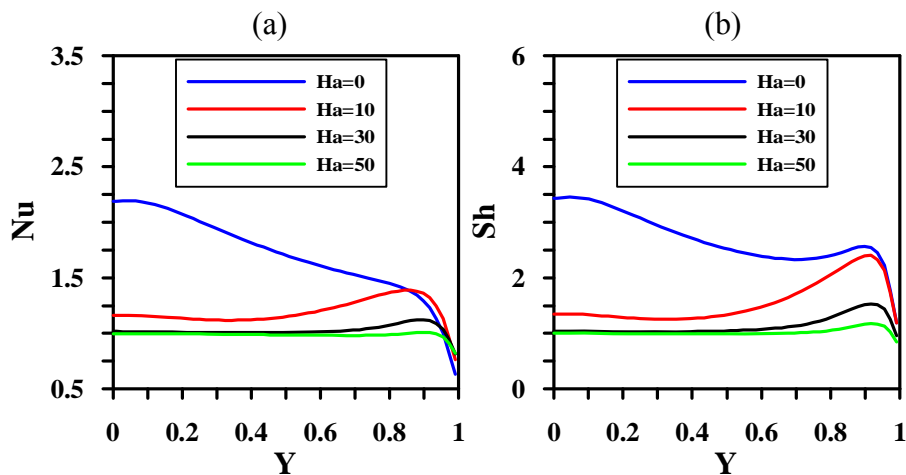


Figure 11: Effect of Hartman number on stream line, isothermals and isoconcentration (upper surface moves to left ($Pr = 0.7, Le = 2, N = 1$ and $Ri=1$)).

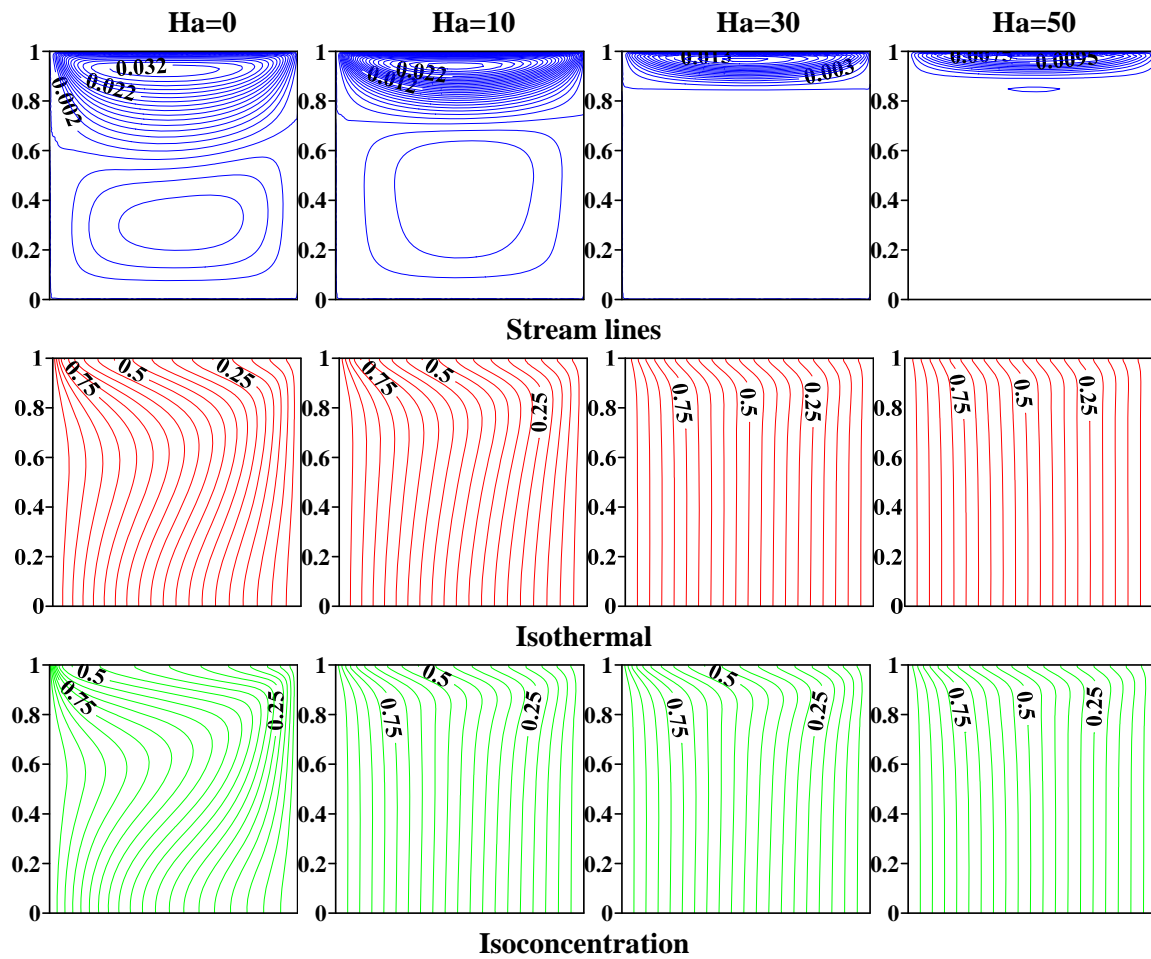


Figure 12: Effect of Hartmann number for (upper surface moves to left, $Pr = 0.7, Le = 2, N = 1$ and $Ri=1$) on (a) Local Nusselt number (b) Local Sherwood number

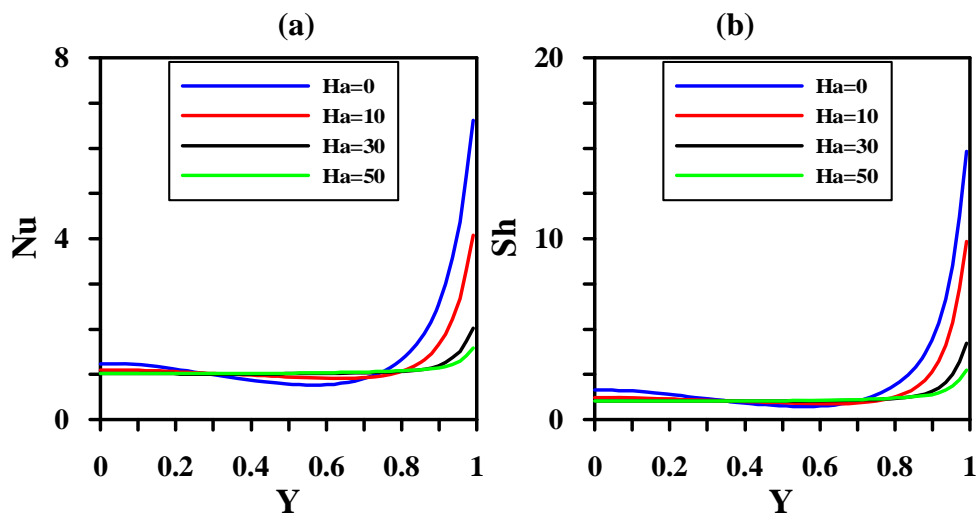


Figure 13: Effect of Hartmann number at different Richardson number, $Pr = 0.7$, $Le = 2$, $N = 1$ on average Nusselt number (a) Upper surface moves right (b) Upper surface moves left

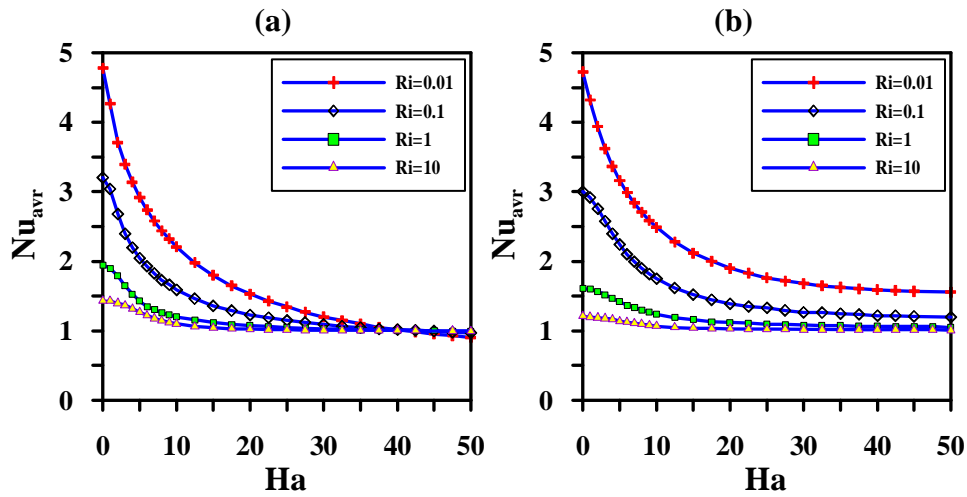
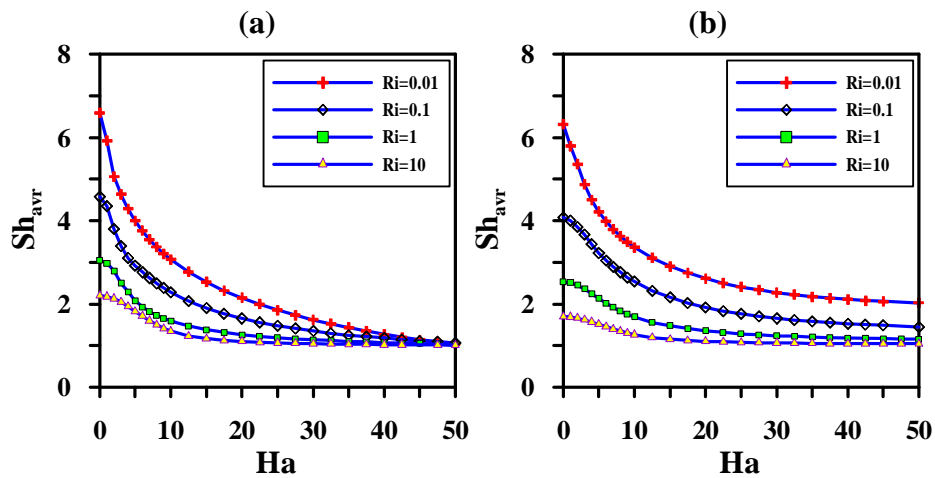


Figure 14: Effect of Hartmann number at different Richardson number, $Pr = 0.7$, $Le = 2$, $N = 1$ on average Nusselt number (a) Upper surface moves right (b) Upper surface moves left



5.3. The Effect of Buoyancy Ratio (N)

5.3.1. Upper Surface Moves to Right

Fig.15 shows the effect of buoyancy ratio on the stream, isothermal and iso-concentration lines at ($Ri=1$, $Ha=10$).The effect of natural convection is on clock wise direction with assisting of the forced convection due to the moving plate to right.

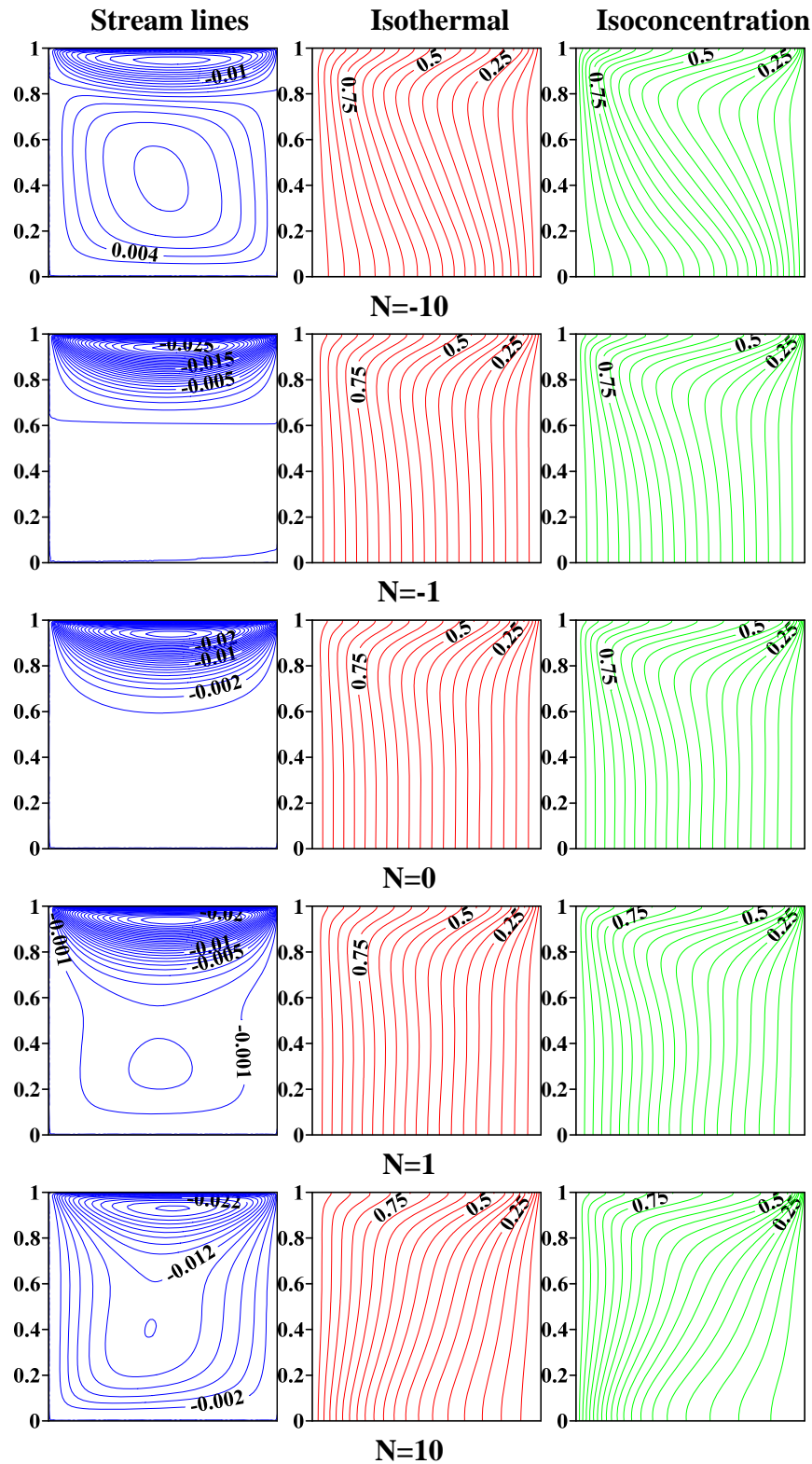
$N > 0$: for all values of N , The stream lines are in clock wise direction by the assistance of natural and forced convection. At $N=1.0$, the solutal and the thermal buoyancy forces are at the same magnitude and the same direction with the forced convection. The flow regime appears as unicell shifted upward near the moving surface due to the effect of magnetic field. At $N=10$, the stream lines spread to fill the whole cavity. The isothermal and iso-concentration inclined more especially at the half bottom of the cavity as the magnitude of the solutal buoyancy increased, as N increases the heat and mass transfer increase.

$N = 0$: normally assisting flow in the cavity in clock wise direction due to the absence of buoyancy ratio effect. The unicell appears near the upper moving surface due to magnetic effect.

$N < 0$: At $N=-10$, two vortices for the streamlines appeared. One of them near the upper surface in clock wise direction due to the effect of forced convection while the second is in the lower part of

the cavity in counter clock wise direction due to the effect of solutal buoyancy force which is ten times the value of thermal buoyancy and opposite in direction.

Figure 15: Effect of bouyancy number on stream line, isothermals and isoconcentration (upper surface moves to right, $Pr= 0.7$, $Ri=1$, $Le=2$, $Ha= 10$).



5.3.2. Upper Surface Moves to Left

The effect of natural convection is on clock wise direction while the forced convection due to the moving plate to left is in opposite direction of natural convection, for the contours shown in Fig.16. At $Ri=1$ (i.e. equivalent effect of both natural and forced convection) so, the buoyancy ratio number has a significant effect on this contours.

$N > 0$: at $N = 1$ the effect of forced convection appears as a vortex in the stream line near the upper surface in counter clockwise direction while both effect of natural and buoyancy ratio appear in large vortex in clock wise direction as the solutal and thermal buoyancy forces are in the same direction. At $N=10$, the upper vortex still appears and shifted up near the upper plate as the effect of the magnetic field is opposite to both solutal and thermal buoyancy forces.

$N < 0$: The effect of solutal buoyancy force is in the opposite direction of thermal buoyancy force and in the same direction of forced flow. As the buoyancy ratio, $N=-10$, the magnitude of the thermal buoyancy force is very small compared with the solutal buoyancy force. The solutal buoyancy force assisting the forced flow and the flow regimes appears as a unicell in the direction of the forced flow. At $N=-1$, the thermal buoyancy force is equal to the solutal buoyancy force in magnitude and in opposite direction. The stream line appears as a cell shifted up near the moving lid and the lower portion of the cavity is stagnant.

$N = 0$: two vortices for the streamlines appeared, as the normal condition. One of them near the upper surface rotates in counter clock wise direction. This is due to the effect of forced convection while the second is in the lower part of the cavity rotates in clock wise direction due to the effect of natural convection in the absence of buoyancy ratio number. The second vortex is weak as the natural convection is in opposite direction to the magnetic field.

5.3.3. Comparison between the Effects of Adding and Opposing Forced on Local Nusselt and Sherwood Number

Figs. 17 and 18. Show the effect of buoyancy ratio at $Ha=10$ and $Ri=1$ on the local Nusselt and Sherwood numbers. For the upper surface moves right, the local Nusselt and Sherwood increases at the lower half of the vertical side and decreases for the upper half of the vertical left side for positive values of N . As for positive values of N , the isothermal and iso-concentration inclined toward right as shown in Fig.(16). For the upper surface moves left, the local Nusselt and Sherwood increases as N decreases for the upper half of the vertical left side. At negative values of N , the solutal buoyancy is in the same direction of forced causing thinner boundary layer at the upper part of the left vertical side for both the isothermal and iso-concentration as shown in Fig. 17. increase heat and mass transfer.

5.4. Comparison between the Effect of Moving Direction of the Upper Surface on Average Nusselt and Sherwood Number

Figs. 19 and 20, Show an important comparison to validate the present study, this comparison is performed at different values of buoyancy ratio and Hartmann number for $Ri=0.01, Ri=1$ to simulate the forced and mixed convection dominated. In the absence of magnetic field, For positive N values, the heat and transfer as the upper surface move to right is greater than as upper surface move to left this due to the assistance between buoyancy ratio and the forced convection reaching maximum value at $N=10$, the increase in heat and mass transfer are 14 and 12% respectively for $Ri=0.01$. for $Ri=1$, respectively for $Ri=0.01$. for $Ri=1$, the increase in heat and mass transfer are 18 and 9% respectively.

Figure 16: Effect of buoyancy number on stream line, isothermals and isoconcentration (upper surface moves to Left, $Pr = 0.7, Ri = 1, Le = 2, Ha = 10$).

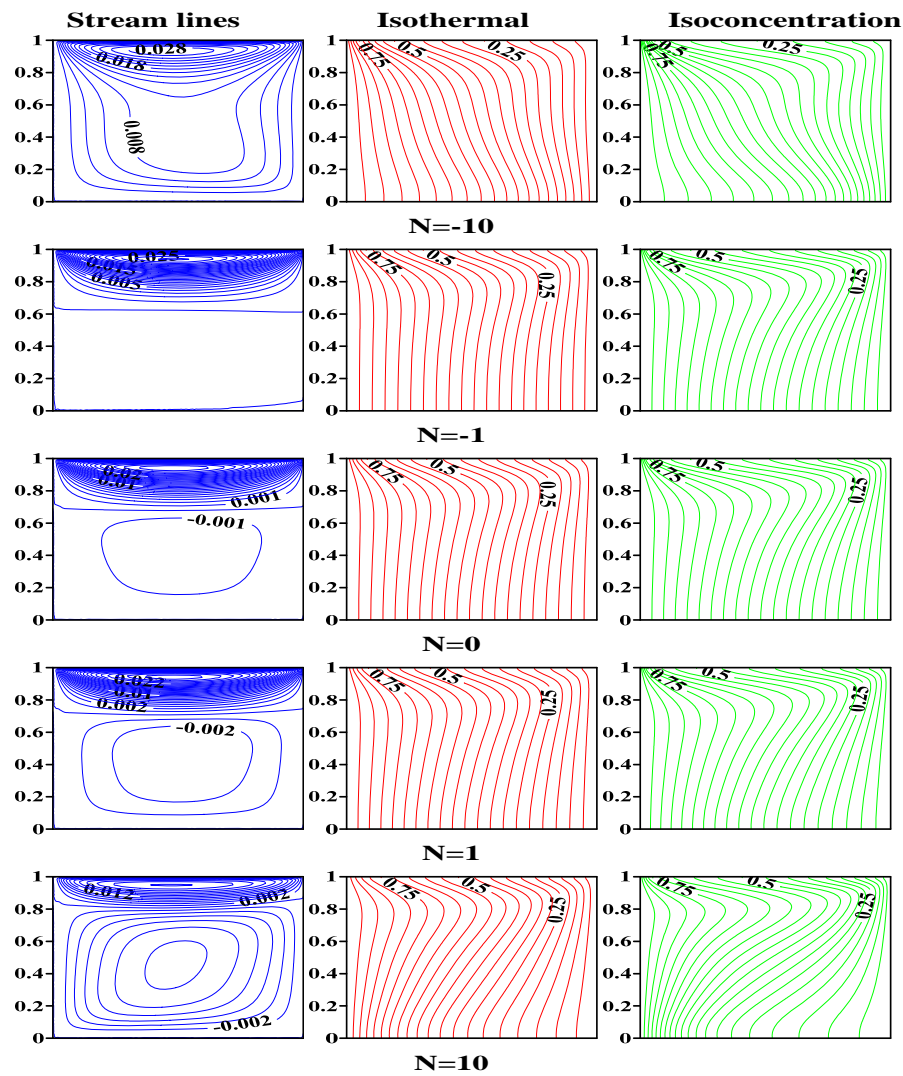


Figure 17: Effect of buoyancy ratio on Local Nusslt number at $Pr = 0.7, Le = 2, Ha = 10$ and $Ri = 1$ on (a) upper surface moves right (b) upper surface moves left

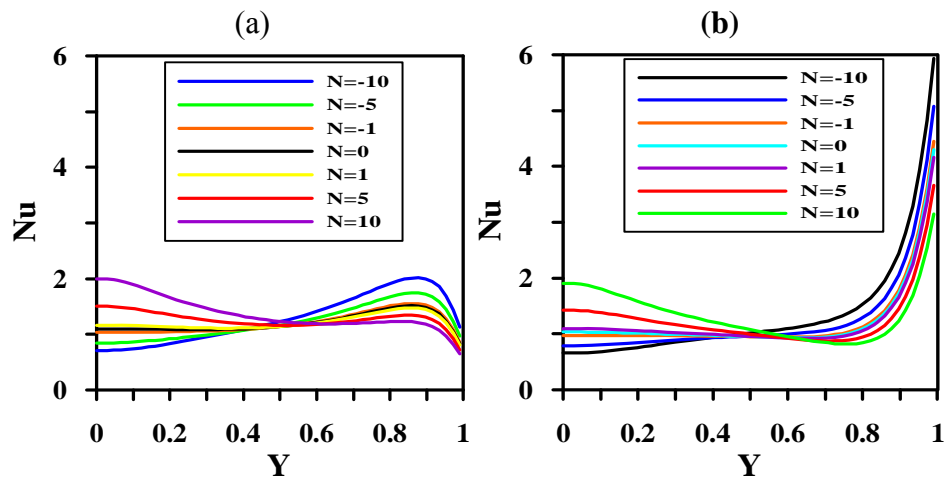
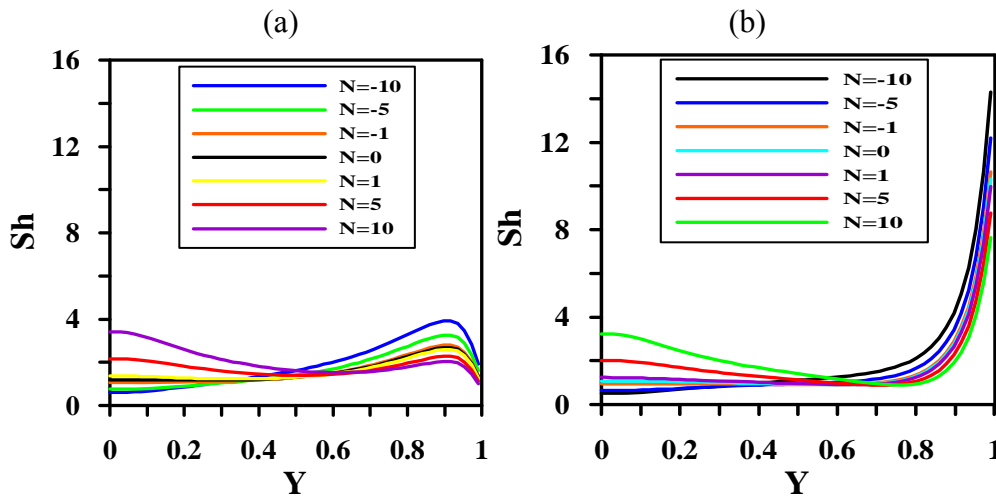


Figure 18: Effect of buoyancy ratio on Local Sherwood number at $Pr = 0.7$, $Le = 2$, $Ha = 10$ and $Ri=1$ on (a) upper surface moves right (b) upper surface moves left



For negative N values the heat transfer as the upper surface move to right is less than as upper surface move to left this due to the opposing between buoyancy ratio and the forced convection. For $Ri=0.01$, The heat and mass transfer increase as the upper surface moves left 29 and 28% respectively than moving to right, while for $Ri=1$, The heat and mass transfer increase are 32 and 21% respectively than moving to right. For $N=-1$, the average Nusselt and Sherwood number are the same for the two direction. As Ha increases, $Ha=10$, the average Nusselt and Sherwood for the upper surface moves left are higher than right to value $N=7$. As Ha increased, the average Nusselt and Sherwood for the upper surface moves left are higher for all values of N.

Figure 19: Effect of buoyancy ratio on average Nusselt number at $Pr = 0.7$, $Le = 2$

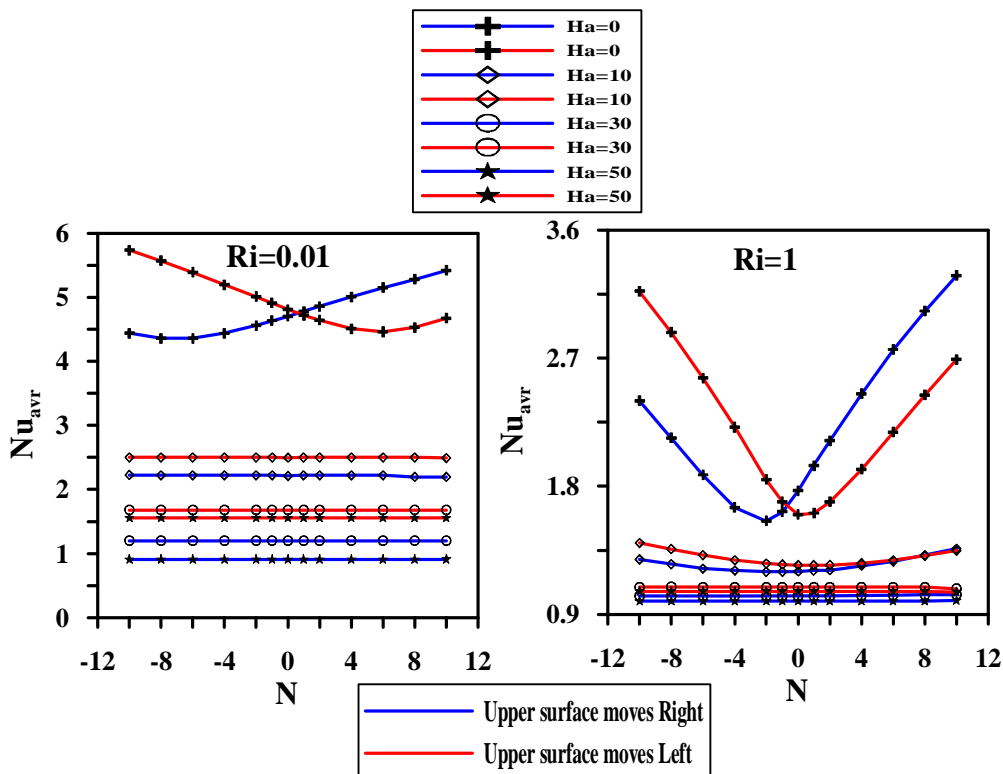
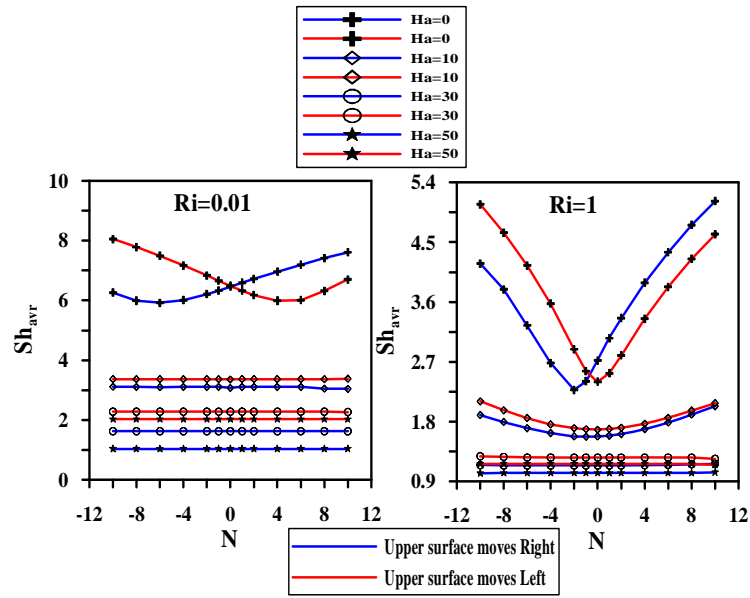


Figure 20: Effect of buoyancy ratio on average Sherwood number at $Pr = 0.7$, $Le = 2$ 

6. Conclusion

- Both heat and mass transfer increased as the Richardson number is decreased, for both upper surface moves to left or to right.
- The heat and mass transfer when upper surface moves right is higher than its value when the upper surface moves to left (opposing flow).
- For forced dominated, as increasing the Hartmann number the heat and mass transfer for the upper surface moves to left is higher than upper surface moves right.
- For mixed dominated, as increasing the Hartmann number the heat and mass transfer for the upper surface moves to left is higher than upper surface moves right.

Nomenclature

B	constant applied magnetic field, Tesla
C	Dimensionless mass concentration
c_h	concentrations at the left wall of the cavity
c_c	concentrations at the right wall of the cavity
D	mass diffusivity, m^2/s
g	acceleration due to gravity, m/s^2
Gr_s	solutal Grashof number
Gr_T	thermal Grashof number
h	heat transfer coefficient, W/m^2K
h_s	Solutal transfer coefficient, W/m^2K
Ha	Hartmann number
k	fluid thermal conductivity, $W/m K$
L	Width of enclosure, m
Le	Lewis number, $Le = \alpha / D$
N	buoyancy ratio, Gr_s / Gr_T
Nu_{avr}	average Nusselt number, $Nu = hL/k$
Nu	Local Nusselt number
P	pressure, N/m^2
Pr	Prandtl number, $Pr = \nu / \alpha$
Re	Reynolds number, $u_o L / \nu$
Ri	Richardson number, Gr / Re^2
Sh_{avr}	average Sherwood number, $Sh = h_s L / D$
Sh	local Sherwood number
T	local temperature, K

T_c	cold wall temperature, K
T_h	hot wall temperature, K
ΔT	temperature difference, $T_h - T_c$, K
U	velocity components in x direction
u_o	movable plate velocity, m/s
V	velocity components in y direction
U	dimensionless velocity component in X direction
V	dimensionless velocity component in Y direction
x, y	dimensional coordinates
X, Y	dimensionless coordinates

Greek Symbols

α	thermal diffusivity, m^2/s
β_T	coefficient of thermal expansion, K^{-1}
β_s	coefficient of solutal expansion, m^3/kg
θ	dimensionless temperature, $(T - T_c)/(T_h - T_c)$
μ	dynamic viscosity, $kg/m\ s$
ν	kinematics viscosity, m^2/s
ρ	local fluid density, kg/m^3
ρ_o	characteristic density, kg/m^3
σ	electrical conductivity

References

- [1] J.W. Lee, J.M. Hyun, 1990, "Double-diffusive convection in a rectangle with opposing horizontal temperature and concentration gradients". *International Journal of Heat and Mass Transfer* 33: 1619-1632.
- [2] A.M. Al-Amiri, K.M. Khanafer, I. Pop, 2007, "Numerical simulation of combined thermal and mass transport in a square lid-driven cavity". *International Journal of Thermal Sciences* 46:662-671.
- [3] M.A.R. Sharif, 2007, "Laminar mixed convection in shallow inclined driven cavities-with hot moving lid on top and cooled from bottom". *Applied Thermal Engineering* 27: 1036-1042.
- [4] C.L. Chen, C.H. Cheng, 2009, "Numerical simulation of periodic mixed convective heat transfer in a rectangular cavity with a vibrating lid". *Applied Thermal Engineering* 29: 2855-2862.
- [5] Khalil M. Khanafer, Abdalla M. Al-Amiri, Ioan Pop, 2007. "Numerical simulation of unsteady mixed convection in a driven cavity using an externally excited sliding lid". *European Journal of Mechanics B/Fluids* 26 : 669–687
- [6] M.M. Rahman, M.A. Alim, M.M.A. Sarker, 2010, "Numerical study on the conjugate effect of joule heating and magneto-hydrodynamics mixed convection in an obstructed lid-driven square cavity". *International Communications in Heat and Mass Transfer* 37:524–534
- [7] Hakan F. Oztop, Khaled Al-Salema, Ioan Pop, 2011, "MHD mixed convection in a lid-driven cavity with corner heater". *International Journal of Heat and Mass Transfer* 54: 3494–3504
- [8] A.J. Chamkha, 2003, "Hydro-magnetic combined convection flow in a vertical lid-driven cavity with internal heat generation or absorption, *Numerical Heat Transfer Part A* 41 : 529–546.
- [9] S. Sivasankaran, A. Malleswaran, J. Lee, P. Sundar, 2011, "Hydro-magnetic combined convection in a lid-driven cavity with sinusoidal boundary conditions on both sidewalls". *International Journal of Heat Mass Transfer* 54 : 512–525.
- [10] T.S. Cheng, 2011, "Characteristics of mixed convection heat transfer in a lid-driven square cavity with various Richardson and Prandtl numbers." *International Journal of Thermal Sciences* 50: 197-205
- [11] H. Ozoe, M. Maruo, 1987, "Magnetic and gravitational natural convection of melted silicon – two dimensional numerical computations for the rate of heat transfer". *JSME* 30 : 774–784.

- [12] T.S. Cheng, W.-H. Liu, 2010,"Effect of temperature gradient orientation on the characteristics of mixed convection flow in a lid-driven square cavity". *Computers & Fluids* 39: 965–978
- [13] Mohamad AA, Viskanta R.,1992,"Laminar flow and heat transfer in Rayleigh–Benard convection with shear". *Phys Fluids A*, 4:2131–40.
- [14] Mohamad AA, Viskanta R.,1994,"Flow structures and heat transfer in a lid-driven cavity filled with liquid gallium and heated from below." *Exp Thermo Fluid Sciences*9:309–19.
- [15] Mohamed A. Teamah, 2008,"Numerical simulation of double diffusive natural convection in rectangular enclosure in the presences of magnetic field and heat source." *International Journal of Thermal Sciences*. 47: 237–248.
- [16] A.J. Chamkha, H. Al-Naser, 2002,"Hydro-magnetic double-diffusive convection in a rectangular enclosure with opposing Temperature and concentration gradients", *International Journal of Heat Mass Transfer* 45 : 2465–2483.
- [17] A.J. Chamkha, H. Al-Naser,2002,"Hydro-magnetic double-diffusive convection in a rectangular enclosure with uniform side heat and mass fluxes and opposing temperature and concentration gradients", *International Journal of Thermal Sciences*. 41 :936–948.
- [18] Changfeng Ma, 2009,"Lattice BGK simulations of double diffusive natural convection in a rectangular enclosure in the presences of magnetic field and heat source", *Nonlinear Anal. Real World Appl.* 10 () 2666-2678.
- [19] Mohamed A. Teamah, Ahmed F. Elsafty, Enass Z. Massoud,2012,"Numerical simulation of double-diffusive natural convective flow in an inclined rectangular enclosure in the presence of magnetic field and heat source", *International Journal of Thermal Sciences* 52 : 161-175
- [20] M. Pirmohammadi, M. Ghassemi, 2009,"Effect of magnetic field on convection heat transfer inside a tilted square enclosure", *International Communications in Heat Mass Transfer* 36: 776-780.
- [21] M. Sathiyamoorthy, A. Chamkha, 2010,"Effect of magnetic field on natural convection flow in a liquid gallium filled square cavity for linearly heated sidewall(s)", *International Journal of Thermal Sciences*49: 1856-865.
- [22] B. Ghasemi, S.M. Aminossadati, A. Raisi, 2011,"Magnetic field effect on natural convection in a nanofluid-filled square enclosure", *International Journal of Thermal Sciences*50:1748-1756.
- [23] M. Venkatachalappa, D. Younghae, M. Sankar, 2011,"Effect of magnetic field on the heat and mass transfer in a vertical annulus", *Int. J. Eng. Sci.* 49 :262-278.
- [24] C. Revnic, T. Grosan, I. Pop, D.B. Ingham, 2011,"Magnetic field effect on the unsteady free convection flow in a square cavity filled with a porous medium with a constant heat generation", *International Journal of Heat Mass Transfer* 54 : 1734-1742.
- [25] M. Zeng, Q.W. Wang, H. Ozoe, 2009,"Natural convection of diamagnetic fluid in an enclosure filled with porous medium under magnetic field", *Prog. Comput. Fluid Dyn.*9: 77-85.
- [26] M. A. Teamah, W. M. El-Maghlany, 2010,"Numerical simulation of double-diffusive mixed convective flow in rectangular enclosure with insulated moving lid", *International Journal of Thermal Sciences* 49 : 1625-1638.
- [27] M. A. Teamah, A. F. Elsafty, M. Z. Elfeky, E. Z. El-Gazzar,2011,"Numerical simulation of double-diffusive natural convective flow in an inclined rectangular enclosure in the presence of magnetic field and heat source, part A: Effect of Rayleigh number and inclination angle", *Alexandria Engineering Journal* 50 : 269-282.
- [28] M A. Teamah and W. M. El-Maghlany,2012," Augmentation of natural convective heat transfer in square cavity by utilizing nano-fluids in the presence of magnetic field and uniform heat generation/absorption" ,*International Journal of Thermal Sciences* 58 :130-142.
- [29] S.V. Patankar, 1980,"*Numerical Heat Transfer and Fluid Flow*". McGRAW-HILL, New York.